MMDJ
MEANDROS MEDICAL AND DENTAL JOURNAL

March 2026 27(1):124-132

Meandros Medical and Dental Journal
doi: 10.69601/meandrosmdj.1746792

Research Article

THE EFFECT OF LASER IRRADIATION WITH DIFFERENT INTENSITIES ON THE SHEAR BOND STRENGTH BETWEEN MINERAL TRIOXIDE AGGREGATE AND GLASS IONOMER CEMENT

Kürşat ER[1], Ömer KIRMALI[2], Serkan ÇINAR[2] Yunus Emre ÇAKMAK[1]* Alper KUSTARCI[1]

[1] Department of Endodontics, Faculty of Dentistry, Akdeniz University, Antalya, TURKIYE

[2] Department of Prosthodontics, Faculty of Dentistry, Akdeniz University, Antalya, TURKIYE

*Correspondence: dt.emrecakmak@gmail.com

Received: *22 July 2025*
Revised: *16 October 2025*
Accepted: *30 October 2025*
Published: *24 March 2026*

Copyright: © 2026 by the authors. Published by Aydın Adnan Menderes University, Faculty of Medicine and Faculty of Dentistry. This article is openly accessible under the Creative Commons Attribution-Non Commercial 4.0 International (CC BY-NC 4.0) License.

ABSTRACT

Objective: This study aimed to evaluate the effects of Erbium, chromium:yttrium-scandium-gallium-garnet (Er,Cr:YSGG) laser irradiation at different energy intensities on the shear bond strength (SBS) between mineral trioxide aggregate (MTA) and glass ionomer cement (GIC).

Materials and Methods: Forty standardized MTA specimens were prepared and stored at 37 °C and 100% humidity for 72 hours. The specimens were randomly divided into four groups (n = 10). The control group received no surface treatment, while the other groups were irradiated with an Er,Cr:YSGG laser at 0.10 W, 0.25 W, or 0.50 W power settings, respectively. Following surface treatment, GIC was applied on all samples in accordance with the manufacturer's instructions. SBS testing was performed using a universal testing machine at a crosshead speed of 0.5 mm/min until failure occurred. The failure modes were assessed under a stereomicroscope at ×32 magnification, and surface morphology was analyzed using scanning electron microscopy (SEM). Data were statistically analyzed using Welch's ANOVA followed by Dunnett's T3 post hoc test with a significance level set at $p < 0.05$.

Results: SBS values differed significantly among groups (Welch ANOVA, p=0.021). The 0.25 W group showed significantly higher SBS than the control, 0.10 W, and 0.50 W groups (Dunnett's T3, p<0.05). No significant differences were found among the control, 0.10 W, and 0.50 W groups.

Conclusion: Er,Cr:YSGG laser irradiation, especially at 0.25 W, enhances the adhesion between MTA and GIC. Laser treatment with optimized parameters may serve as an effective surface modification method to improve bonding.

Keywords: Bioceramic Materials; Surface Modification; ErCr:YSGG Laser; Shear Bond Strength; Glass Ionomer Cement

MMDJ
MEANDROS MEDICAL AND DENTAL JOURNAL
March 2026 27(1):124-132
Meandros Medical and Dental Journal
doi: 10.69601/meandrosmdj.1746792

INTRODUCTION

Mineral Trioxide Aggregate (MTA) was first developed by Torabinejad in 1993 for use as a retrograde filling material and has subsequently established itself as a fundamental component in contemporary endodontic practice (1,2). The primary constituents of MTA include tricalcium and dicalcium silicate compounds, which provide excellent biocompatibility characteristics and superior sealing properties (3). Clinical applications of MTA encompass furcation perforation management, internal resorption therapy, pulpotomy procedures, and pulp capping treatments for both reversible and irreversible pulpitis conditions. Additionally, MTA serves as a preferred root canal obturation material, demonstrating its essential position within modern endodontic treatment modalities (4,5).

In recent years, minimally invasive approaches and vital pulp therapies have become increasingly important, with an emphasis on preserving pulp vitality. Accordingly, the use of MTA in pulp capping, direct pulp capping, and pulpotomy has expanded. A primary driver of this trend is the superior dentinogenic capacity of MTA compared to calcium hydroxide, resulting in faster and more effective healing of the pulp tissue (3,6). Studies (7,8) have shown that MTA promotes better dentin bridge formation and biocompatibility, making it a highly valuable material for vital pulp therapies. Particularly in line with contemporary approaches focused on pulp preservation, the application areas of MTA continue to expand, further establishing its central role in endodontic protocols (7,9,10). Despite its favorable properties, such as superior biocompatibility, dentinogenesis induction, and antimicrobial characteristics, MTA has certain notable disadvantages (11). These drawbacks include a prolonged setting time, a tendency for high solubility during the setting process, potential for discoloration which is considered an aesthetic limitation and difficulties in handling (11,12). In particular, when MTA is used as a pulp capping material, its extended setting time may necessitate additional clinical sessions, posing a disadvantage in endodontic practice (11,13).

Although newer, faster-setting MTA derivatives have been introduced to address the drawback of prolonged setting times, their clinical efficacy and sealing properties are still being evaluated (14). Traditionally, the use of an intermediate material such as glass ionomer cement (GIC) was considered to facilitate the placement of the final restoration before MTA is fully set (15). However, recent studies have demonstrated that immediate placement of GIC over freshly mixed MTA can adversely affect the hydration and setting process of the underlying material, resulting in increased porosity and microcracks at the interface (16).

In current clinical practice, a two-visit approach is sometimes employed in situations such as pulpal exposures, furcal repairs, or in pediatric patients who require behavioral management (17). In these cases, MTA is allowed to fully set before the final restoration is placed. Recent evidence, however, emphasizes that delayed placement of a resin composite restoration with a universal adhesive over fully set calcium silicate-based materials offers superior bond strength and mechanical compatibility compared to GIC (18).

While direct placement of resin composite restorations over fully set MTA represents current standard practice, specific clinical scenarios—such as uncooperative pediatric patients or unavoidable multi-visit protocols—may still necessitate GIC application as an intermediate base (19). Accordingly, this study simulates a delayed restoration protocol to investigate whether laser conditioning can enhance the bonding performance between fully set MTA and GIC. Although recent research demonstrates that resin composites with universal adhesives achieve superior bond strength to MTA compared to GIC when delayed restoration is feasible (13,16,20), optimizing the MTA-GIC interface remains clinically relevant for situations where GIC serves as a protective base, potentially creating a "double seal" effect and contributing to pulp-dentin complex preservation.

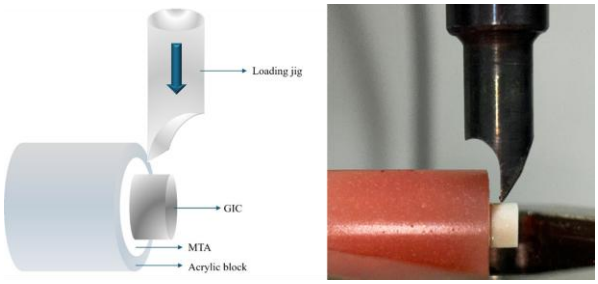


Figure 1. Experimental setup for shear bond testing and laser irradiation. (A) schematic of loading jig and specimen geometry; (B) actual setup photograph.

GICs are widely used in restorative dentistry due to their chemical adhesion to tooth structure, fluoride release, and moisture tolerance (21). While direct resin composite application over freshly mixed MTA presents clinical challenges—including potential interference with MTA setting and displacement during etching procedures—

MMDJ
MEANDROS MEDICAL AND DENTAL JOURNAL
March 2026 27(1):124-132
Meandros Medical and Dental Journal
doi: 10.69601/meandrosmdj.1746792

GIC placement over partially set MTA has been recommended as an alternative approach (21,22). However, limited research exists on enhancing the bond strength between MTA and conventional GIC. The differing chemical and physical properties of these materials create challenges in achieving optimal adhesion, prompting investigation of surface treatment procedures such as laser irradiation to improve interfacial bonding.

Therefore, the purpose of this study was to evaluate the effect of Er,Cr:YSGG laser surface conditioning at three different power settings (0.10 W, 0.25 W, and 0.50 W) on the shear bond strength between fully set MTA and conventional GIC. The specific objectives were: to measure and compare the shear bond strength values of laser-treated groups versus untreated controls; to analyze the failure modes of debonded specimens using stereomicroscopy; and to characterize the surface morphological changes of laser-conditioned MTA using scanning electron microscopy (SEM). The null hypothesis stated that Er,Cr:YSGG laser surface modification would not significantly alter the shear bond strength at the MTA-GIC interface regardless of the applied power parameters. It should be recognized that the clinical relevance of this protocol is limited to scenarios where delayed GIC restoration is necessary and direct composite restoration is not immediately feasible.

MATERIALS AND METHODS

The materials used in this study were white MTA (Angelus MTA, Angelus, Londrina, Brazil) and capsule-form GIC (GC Fuji IX GP® FAST, GC Corp., Tokyo, Japan). The material composition and manufacturer details are provided in Table 1. Ethical approval was not required for this in vitro study as no human participants or animals were involved.

A priori power analysis using G*Power software ($\alpha = 0.05$, power = 0.80, effect size f = 0.80, 4 groups) determined a minimum sample size of 10 specimens per group.

Preparation of MTA Specimens

Forty MTA test specimens were fabricated utilizing cylindrical acrylic molds measuring 4 mm in diameter and 2 mm in height. The MTA material was prepared following manufacturer guidelines and introduced into the mold cavities using a carrier instrument, followed by condensation with a plugger tool. Surplus material was subsequently eliminated from the specimen surfaces using a scraper instrument. Following MTA placement within the acrylic templates, surface leveling was accomplished using a stainless-steel spatula to achieve consistent flatness and uniformity across all samples (Figure 1). The completed specimens were maintained under moist cotton pellet coverage and incubated at 37°C under saturated humidity conditions for 72 hours. Following the setting period, specimen surfaces were uniformly prepared using 600-grit silicon carbide sandpaper with continuous water cooling. Subsequently, specimens were randomly allocated into four experimental groups (n = 10) based on the applied surface conditioning protocols:
Control Group: No surface treatment procedure was applied.
Laser Irradiation Groups (0.10, 0.25, 0.50 W).

The bonding surfaces of set MTA were irradiated with an Er,Cr:YSGG laser (Millennium; Biolase Technology, San Clemente, CA, USA; $\lambda = 2.78$ μm) delivered through a 600 μm MZ6 plain fiber tip (tip transmission factor = 0.75). Three power settings were used: 0.10 W (10 mJ/pulse), 0.25 W (25 mJ/pulse), and 0.50 W (50 mJ/pulse) at 10 Hz with a 140 μs pulse duration. The tip was positioned 10 mm from the surface in non-contact mode and activated for 20 s with

Table 1. Materials used in the study

Material/Equipment	Manufacturer	Type/Model	Composition/Specifications	LOT Number
White MTA	Angelus, Londrina, Brazil	MTA-Angelus	Silicon oxide, potassium oxide, aluminum oxide, iron oxide, calcium oxide, bismuth oxide, sodium sulfate, crystalline silica particles	3343
Glass Ionomer Cement	GC Corp., Tokyo, Japan	GC Fuji IX GP® FAST (Type 2 Restorative GIC)	Distilled water, polybasic carboxylic acid, fluoro-alumino-silicate glass, pigments	06161
Er,Cr:YSGG Laser	Biolase Technology, San Clemente, CA, USA	Millennium	$\lambda = 2.78$ μm; 600 μm MZ6 plain fiber tip (tip transmission factor: 0.75)	-
Silicon Carbide Paper	-	600-grit	Wet grinding	-
Acrylic Resin	-	Cold-cure	Mounting blocks	-
Silicone Molds	-	Cylindrical	3 mm internal diameter × 4 mm height	-

MMDJ
MEANDROS MEDICAL AND DENTAL JOURNAL
March 2026 27(1):124-132
Meandros Medical and Dental Journal
doi: 10.69601/meandrosmdj.1746792

circular scanning motion to ensure uniform coverage of the entire MTA surface (4 mm diameter, 0.126 cm² area). The total energy delivered and corresponding energy densities were: 2 J and 15.9 J/cm² (0.10 W), 5 J and 39.7 J/cm² (0.25 W), and 10 J and 79.4 J/cm² (0.50 W), respectively. Water/air cooling was maintained at 50% throughout the irradiation process.

Following surface treatment procedures, encapsulated GIC was applied to all forty specimens as described below. After SBS testing and specimen debonding, failure mode classification was performed on all 40 specimens using stereomicroscopy (Zeiss, Jena, Germany) at 32× magnification immediately after mechanical testing. The failure modes were categorized into three distinct types: adhesive failure, characterized by complete separation of the GIC from the MTA substrate; cohesive failure, involving complete fracture within the GIC material itself; and mixed failure, exhibiting characteristics of both adhesive and cohesive failure mechanisms. Subsequently, one debonded specimen from each experimental group was randomly selected for detailed scanning electron microscopy (SEM) analysis to further characterize the fracture interface and surface morphology. Failure-mode distribution was recorded for all 40 specimens under stereomicroscopy immediately after testing. SEM imaging was performed on one representative specimen per group for qualitative surface characterization and did not alter the mechanical testing sample size (n=10/group).

Placement of the GIC

Following completion of surface conditioning procedures, encapsulated GIC was prepared using mechanical mixing via amalgamator in accordance with manufacturer specifications. The prepared GIC material was subsequently dispensed onto the central region of each MTA specimen using a dedicated applicator instrument. Standardized cylindrical silicone molds (3 mm internal diameter × 4 mm height) were positioned perpendicularly on the MTA surface to control GIC specimen geometry. These molds were carefully removed after 10 minutes using gentle rotational lifting movements to minimize interfacial stress and ensure adequate initial setting. The fabricated MTA-GIC composite specimens underwent storage at 37°C under complete humidity saturation for 72 hours prior to SBS evaluation. Before mechanical testing, all specimens were embedded within custom-fabricated acrylic resin mounting blocks to ensure stable specimen orientation and eliminate movement artifacts during SBS assessment.

SEM analysis

Following SBS testing, one debonded specimen from each experimental group was randomly selected for high-resolution surface characterization using scanning electron microscopy (SEM) (JSM-6060LV, JEOL, Tokyo, Japan). The selected specimens were sputter-coated with gold-palladium and examined at ×500 and ×1000 magnifications to evaluate the surface morphology of laser-treated MTA and to characterize the fracture interfaces. This post-debonding SEM analysis allowed detailed assessment of surface topographical changes induced by different laser parameters and their relationship to failure patterns, without affecting the sample size used for statistical analysis (n=10 per group). For illustrative purposes, representative SEM images included in the manuscript were captured at ×150 magnification to provide a general overview of the surface features, while detailed analyses were performed at higher magnifications.

Shear bond strength test

SBS evaluation was performed using a universal testing machine (Lloyd LF Plus, Ametek Inc., Lloyd Instruments, Leicester, UK) with a crosshead displacement rate of 0.5 mm/min applied continuously until adhesive failure was achieved. The maximum failure force was documented in Newtons and subsequently converted to calculate SBS values expressed in Megapascals (MPa).

Statistical analysis

Statistical evaluation utilized SPSS version 24.0 (SPSS Inc, Chicago, IL, USA). Data normality was verified using the Shapiro-Wilk test, confirming normal distribution across all experimental conditions ($p>0.05$). Levene's test was performed to assess homogeneity of variance. Since the assumption of equal variances was violated (Levene statistic=6.119, $p=0.002$), Welch's ANOVA was employed as a robust alternative to one-way ANOVA for comparing bond strength among groups. Pairwise comparisons were performed using Dunnett's T3 post hoc test, which does not assume equal variances. Effect size was calculated using eta-squared (η^2) to evaluate the magnitude of treatment effects. Data are presented as mean ± standard deviation, with statistical significance set at $\alpha = 0.05$.

RESULTS

Table 2 displays the mean shear bond strength values, standard deviations, and ranges across all treatment groups. Levene's test indicated heterogeneity of variance

MMDJ
MEANDROS MEDICAL AND DENTAL JOURNAL
March 2026 27(1):124-132
Meandros Medical and Dental Journal
doi: 10.69601/meandrosmdj.1746792

among groups (p=0.002); therefore, Welch's ANOVA was applied, revealing statistically significant differences in SBS among the experimental groups (Welch F=4.108, df=3,19.412, p=0.021). The effect size was substantial (η^2=0.42), indicating that approximately 42% of the variance in bond strength was attributable to the laser treatment protocol. Dunnett's T3 post hoc analysis demonstrated that the 0.25 W group exhibited significantly higher bond strength (7.07 ± 2.18 MPa) compared to the control (4.44 ± 0.92 MPa, p=0.023), 0.10 W (4.58 ± 0.81 MPa, p=0.032), and 0.50 W (4.47 ± 1.12 MPa, p=0.028) groups. No significant differences were observed among the control, 0.10 W, and 0.50 W groups.

Table 2. Shear bond strength (SBS) of the MTA–GIC interface at different laser powers (0.10, 0.25, 0.50 W): mean ± SD (MPa) and Min–Max (n=10/group).

Groups	n	Mean ± SD (MPa)	Min–Max
Control	10	4.44 ± 0.92[a]	3.21–5.89
0.10 W	10	4.58 ± 0.81[a]	3.45–5.76
0.25 W	10	7.07 ± 2.18[b]	4.22–10.15
0.50 W	10	4.47 ± 1.12[a]	2.98–6.34

Failure mode analysis demonstrated that fractures occurred predominantly as adhesive failures at the MTA/GIC interface, accounting for 70% of all failures. Mixed failure patterns were observed in 30% of cases, while cohesive failures within the GIC were not detected in any specimens.

SEM evaluation of MTA surface topography revealed irregular surfaces with melting and pit formation (indicated by white arrows in Figure 2C) following laser irradiation at different intensities, compared to untreated control samples. It was observed that after the removal of the water required for the hardening of the MTA with high laser energy, carbonized areas were formed on the surface of the MTA that would disrupt the bonding with the GIC and also in the 0.25 W laser applied groups, irregular areas on the MTA surface were monitored (Figure 2C).

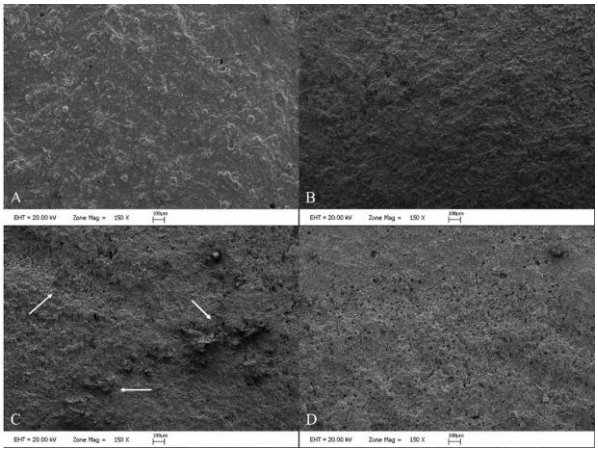


Figure 2. Representative SEM images of debonded MTA surfaces following SBS testing. A; Control group showing untreated MTA surface, B; Surface morphology following 0.10W laser irradiation, C; Surface topography following 0.25W laser irradiation showing carbonized areas and micro-pits (white arrows), D; Surface alterations following 0.50W laser irradiation demonstrating excessive ablation.

DISCUSSION

The present study evaluated the effect of Er,Cr:YSGG laser surface conditioning on the shear bond strength between fully set MTA and conventional GIC. The findings demonstrated that laser irradiation at 0.25 W significantly increased SBS compared to the control group (7.07 ± 2.18 vs 4.44 ± 0.92 MPa; $p < 0.05$), representing an approximately 59% improvement in bond strength. In contrast, the 0.10 W and 0.50 W groups showed no significant improvement compared to controls. Therefore, the null hypothesis was rejected. Importantly, 70% of failures across all groups occurred at the MTA-GIC interface (adhesive failure), indicating that the primary challenge lies in establishing reliable bonding between these dissimilar materials rather than cohesive failure within either material.

The superior performance of the 0.25 W laser group can be attributed to the creation of an optimally modified surface topography that enhanced micromechanical retention without compromising MTA's structural integrity. SEM analysis revealed that this power setting produced uniform micro-irregularities and shallow crater-like features across the MTA surface, increasing the available surface area for GIC penetration and mechanical interlocking. These surface modifications likely facilitated improved wetting and adaptation of the polyalkenoic acid component of GIC, promoting both mechanical retention and potential chemical interaction sites between carboxyl groups and calcium ions released from the modified MTA surface (13,22).

Furthermore, the 0.25 W setting appears to represent an ideal balance between achieving sufficient surface activation to promote bonding while maintaining the underlying structural integrity of the calcium silicate hydrate matrix (23,24). The moderate energy density at this power level may have selectively removed loosely bound surface particles and exposed reactive calcium silicate phases without inducing thermal damage or extensive microcracking that could weaken the interface. The relatively high standard deviation observed in this group suggests some variability in surface response,

possibly related to inherent heterogeneity in MTA surface composition or localized differences in laser-material interaction (24).

The lack of significant improvement in the 0.10 W laser group compared to controls suggests that this power setting delivered insufficient energy to meaningfully alter the MTA surface. SEM examination revealed minimal topographical changes, with the surface remaining relatively smooth and similar to untreated controls. This inadequate surface modification failed to create sufficient micromechanical retention sites or expose reactive chemical groups necessary for enhanced GIC adhesion (25, 26). The predominantly adhesive failure pattern in this group (similar to controls) confirms that the interface remained the weakest point, indicating that low-power laser treatment alone is insufficient to overcome the inherent bonding challenges between set MTA and GIC.
In contrast, the 0.50 W laser group demonstrated no improvement—bond strength values remained nearly identical to untreated controls—despite markedly different surface morphology. SEM analysis revealed excessive surface ablation characterized by deep craters, irregular cavitations, and evidence of thermal damage including carbonization and microfracturing of the MTA surface. This over-treatment likely compromised the structural integrity of the superficial MTA layer, creating a weakened zone susceptible to cohesive failure. Additionally, the extreme surface roughness and thermal alterations may have impeded proper GIC adaptation and flow into surface irregularities, thereby reducing effective contact area and chemical interaction potential (18). The persistent high rate of adhesive failures in this group suggests that excessive energy delivery disrupts rather than enhances the bonding interface, negating any potential benefit from increased surface roughness.

The observed surface alterations and their differential effects on bond strength can be explained by the fundamental mechanisms of Er,Cr:YSGG laser-tissue interaction. The 2.78 μm wavelength of this laser corresponds to a strong absorption peak of water molecules present in the hydrated MTA structure. At the optimal energy density of 39.7 J/cm² (0.25 W group), the absorbed laser energy induces rapid microexplosions as water molecules vaporize, creating controlled surface ablation that produces uniform micro-irregularities without excessive thermal accumulation (27). This process, known as photothermal ablation, selectively removes loosely bound surface particles while exposing underlying reactive calcium silicate phases. However, at higher energy density (79.4 J/cm², 0.50 W group), prolonged energy exposure exceeds the thermal relaxation time of the material, leading to progressive dehydration of the MTA surface layer. Once the water content is depleted, continued laser irradiation results in direct heating and thermal decomposition of the calcium silicate matrix, manifesting as carbonization—evidenced by the dark, charred appearance observed in SEM images. This carbonized layer, characterized by reduced surface energy, hydrophobicity, and chemical inertness, prevents effective wetting by the hydrophilic GIC and blocks potential ionic interactions between carboxyl groups and calcium ions. Conversely, insufficient energy density (15.9 J/cm², 0.10 W group) fails to exceed the ablation threshold of the MTA surface, resulting in minimal morphological changes. These findings underscore the critical importance of precise energy parameter selection to achieve beneficial surface modification while avoiding detrimental thermal effects that compromise bonding potential.

Previous investigations of MTA surface treatments have explored various approaches including acid-etching (28,29), hydrofluoric acid with silane application (30), and polyacrylic acid conditioning (31), with mixed results. However, evidence regarding laser pretreatment for MTA-restorative material bonding remains limited. The present findings extend this literature by demonstrating that optimal laser parameters can substantially improve GIC adhesion to fully set MTA.

The bond strength values achieved in the optimal 0.25 W group substantially exceed those reported by Palma et al. (16,18) for conventional GIC-MTA bonding (approximately 1.2 MPa). However, their studies also demonstrated that delayed composite placement with universal adhesives achieved bond strengths of approximately 6.0 MPa, which remain comparable to our optimized laser-GIC protocol. This suggests that while laser conditioning can substantially improve GIC adhesion to MTA, resin-based restoration with appropriate bonding protocols still represents the preferred approach when clinically feasible.
The control group bond strength in the present study is notably higher than values reported by Palma et al. (16,18), which may be attributed to methodological differences including specimen preparation, GIC formulation, storage conditions (32, 33), or testing protocols. Despite these baseline differences, the relative improvement achieved through optimal laser conditioning (~59%) demonstrates the potential clinical utility of this surface treatment approach.

MMDJ
MEANDROS MEDICAL AND DENTAL JOURNAL
March 2026 27(1):124-132
Meandros Medical and Dental Journal
doi: 10.69601/meandrosmdj.1746792

The predominance of adhesive failures observed in this study is consistent with findings from previous investigations (18,34), which attributed poor MTA-GIC bonding to the crystalline, hydrophilic, and chemically inert nature of fully set calcium silicate cement surfaces. While laser conditioning at 0.25 W improved mechanical retention, it did not fundamentally alter the chemical incompatibility between these materials, as evidenced by the continued prevalence of interfacial failures. Xavier et al. (34) similarly emphasized that additional intermediate bonding layers could improve interfacial compatibility, supporting the rationale for surface optimization strategies.

From a clinical perspective, these findings suggest that Er,Cr:YSGG laser conditioning at 0.25 W may provide clinically meaningful improvement in GIC adhesion to fully set MTA in scenarios where delayed restoration is unavoidable—such as multi-visit treatments for uncooperative pediatric patients or complex perforation repairs (19). However, it must be emphasized that this protocol does not represent current standard care, as immediate composite restoration with appropriate bonding protocols consistently achieves superior outcomes (18).

Several limitations warrant consideration. This in vitro study employed static loading conditions that do not replicate the dynamic masticatory forces, thermal cycling, and moisture exposure encountered in the oral environment. The specimen dimensions and 72-hour setting period were selected based on established protocols (13, 32, 33, 35), yet do not reflect the increasingly favored immediate restoration approach. Additionally, the assessment was limited to conventional GIC; resin-modified GIC or other intermediate materials may respond differently to laser conditioning. The relatively high standard deviation in the 0.25 W group suggests that achieving consistent surface modification may require careful calibration and technique standardization in clinical applications. Future investigations should evaluate the long-term durability of laser-conditioned interfaces under simulated clinical conditions and compare various restorative material combinations.

CONCLUSION

This study demonstrated that Er,Cr:YSGG laser conditioning at 0.25 W significantly improved the shear bond strength between fully set MTA and conventional GIC by approximately 59% compared to untreated controls (7.07 vs 4.44 MPa; $p < 0.05$). This improvement was achieved through the creation of optimal surface micro-irregularities that enhanced micromechanical retention without causing thermal damage. Lower power (0.10 W) produced insufficient surface modification, while higher power (0.50 W) caused detrimental carbonization and microcracking. However, the predominance of adhesive failures (70%) indicates persistent chemical incompatibility between these materials despite mechanical enhancement. Within the limitations of this in vitro investigation, optimized laser treatment may offer a viable surface conditioning approach when GIC is clinically required as an intermediate base over fully set MTA in delayed restoration protocols.

Acknowledgments
The authors would like to acknowledge that this study was presented as an abstract at the 9th International Symposium of the Turkish Society of Endodontics, held in Mardin, Turkey, between May 19 and 22, 2022 (abstract published on pp. 350–351 of the symposium proceedings).

Authorship contributions
K.E.: Conceptualization, Methodology, Supervision, Validation, Visualization, Writing – Original Draft, Writing – Review and Editing. Ö.K.: Conceptualization, Data Curation, Investigation, Methodology, Visualization, Validation, Writing – Original Draft. S.Ç.: Methodology, Validation. Y.E.Ç.: Methodology, Writing – Review and Editing. A.K.: Methodology, Validation, Writing – Original Draft.

Data availibity statement
The data that support the findings of this study are available from the corresponding author upon reasonable request.

Declaration of competing interest
The authors declare that there is no conflict of interest related to this study.

Ethics
Ethical approval was not required for this in vitro study as no human participants or animals were involved.

Funding
This research received no specific grant from any funding agency in the public, commercial, or not-for-profit sectors.

REFERENCES

1. Torabinejad M, Chivian N. Clinical applications of mineral trioxide aggregate. J Endod 1999; 25: 197-205.

2. Torabinejad M, Watson TF, Pitt Ford TR. Sealing ability of a mineral trioxide aggregate when used as a root end filling material. J Endod 1993; 19: 591-5.
3. Çakmak YE, Erkal D, Er K. Vital pulpa tedavilerinde biyoseramiklerin kullanımı. In: Yiğit Özer SG, editör. Endodontide Biyoseramik. 1. Baskı. Ankara: Türkiye Klinikleri; 2025: 9-24.
4. Kaur M, Singh H, Dhillon JS, Batra M, Saini M. MTA versus Biodentine: review of literature with a comparative analysis. J Clin Diagn Res 2017; 11: ZG01-5.
5. Prakash V, Darsini HJ, Karthick A, Venkatesh A, Darsini H. Mineral trioxide aggregate (MTA) - an overview. Eur J Mol Clin Med 2020; 7: 2115-2120.
6. Çakmak YE, Er K. Clinical Applications of Mineral Trioxide Aggregate in Endodontics: A Case Series. Dentistry Kazakhstan 2024; (3): 4-14.
7. Leye Benoist F, Gaye Ndiaye F, Kane AW, Benoist HM, Farge P. Evaluation of mineral trioxide aggregate (MTA) versus calcium hydroxide cement (Dycal) in the formation of a dentine bridge: a randomised controlled trial. Int Dent J 2012; 62: 33-9.
8. Hilton TJ, Ferracane JL, Mancl L. Comparison of CaOH with MTA for direct pulp capping: a PBRN randomized clinical trial. J Dent Res 2013; 92: S16-22.
9. Taneja S, Singh A. Evaluation of effectiveness of calcium hydroxide and MTA as pulpotomy agents in permanent teeth: a meta-analysis. Pediatric Dent J 2019; 29: 90-6.
10. Mente J, Hufnagel S, Leo M, Michel A, Gehrig H, Panagidis D, et al. Treatment outcome of mineral trioxide aggregate or calcium hydroxide direct pulp capping: long-term results. J Endod 2014; 40: 1746-51.
11. Dawood AE, Parashos P, Wong RHK, Reynolds EC, Manton DJ. Calcium silicate-based cements: composition, properties, and clinical applications. J Investig Clin Dent 2017; 8: e12195.
12. Camilleri J. Staining potential of Neo MTA Plus, MTA Plus, and Biodentine used for pulpotomy procedures. J Endod 2015; 41: 1139-45.
13. Yesilyurt C, Yildirim T, Taşdemir T, Kusgoz A. Shear bond strength of conventional glass ionomer cements bound to mineral trioxide aggregate. J Endod 2009; 35: 1381-3.
14. Xavier MT, Costa AL, Ramos JC, Caramês J, Marques D, Martins JNR. Calcium Silicate-Based Cements in Restorative Dentistry: Vital Pulp Therapy Clinical, Radiographic, and Histological Outcomes on Deciduous and Permanent Dentition—A Systematic Review and Meta-Analysis. Materials 2024; 17: 4264.
15. Tsujimoto M, Tsujimoto Y, Ookubo A, Shiraishi T, Watanabe I, Yamada S, Hayashi Y. Timing for composite resin placement on mineral trioxide aggregate. J Endod. 2013 Sep;39(9):1167-70. doi: 10.1016/j.joen.2013.06.009.
16. Palma PJ, Marques JA, Falacho RI, Vinagre A, Santos JM, Ramos JC. Does Delayed Restoration Improve Shear Bond Strength of Different Restorative Protocols to Calcium Silicate-Based Cements? Materials 2018; 11: 2216.
17. Daniele L. Mineral trioxide aggregate (MTA) direct pulp capping: 10 years clinical results. Giornale Italiano di Endodonzia. 2017;31(1):48-57.
18. Palma PJ, Marques JA, Antunes M, et al. Effect of restorative timing on shear bond strength of composite resin/calcium silicate–based cements adhesive interfaces. Clin Oral Invest 2021; 25: 3131-3139.
19. Hatipoğlu FP, Hatipoğlu Ö, Taha N, Lehmann AP, Aldhelai TA, Madfa AA, et al. Attitude and practice of regenerative endodontic procedures among endodontists and paediatric dentists: A multinational survey from 13 countries. Int J Paediatr Dent 2023; 33: 521-534.
20. Yanık D, Er K, Kuştarci A. Shear bond strength of resin-modified glass ionomer cement bound to mineral trioxide aggregate after various disinfection protocols. Aust Endod J 2023; 49: 159-64.
21. Nandini S, Ballal S, Kandaswamy D. Influence of glass-ionomer cement on the interface and setting reaction of mineral trioxide aggregate when used as a furcal repair material using laser Raman spectroscopic analysis. J Endod 2007; 33: 167-72.
22. Ballal S, Venkateshbabu N, Nandini S, Kandaswamy D. An in vitro study to assess the setting and surface crazing of conventional glass ionomer cement when layered over partially set mineral trioxide aggregate. J Endod 2008; 34: 478-80.
23. Dong X, Xu X. Bioceramics in endodontics: updates and future perspectives. Bioengineering (Basel) 2023; 10: 354.
24. Stringhini Junior E, Dos Santos MGC, Oliveira LB, Mercadé M. MTA and biodentine for primary teeth pulpotomy: a systematic review and meta-analysis of clinical trials. Clin Oral Investig 2019; 23: 1967-1976.
25. Nicholson JW. Adhesion of glass-ionomer cements to teeth: a review. Int J Adhes Adhes 2016; 69: 33-38.
26. Zheng B, Cao S, Al-Somairi MAA, He J, Liu Y. Effect of enamel-surface modifications on shear bond strength using different adhesive materials. BMC Oral Health 2022; 22: 224.
27. Lagunov VL, Rybachuk M, Itthagarun A, Walsh LJ, George R. Modification of dental enamel, dentin by an ultra-fast femtosecond laser irradiation: a systematic review. Optics & Laser Technology. 2022;155:108439.
28. Kayahan MB, Nekoofar MH, Kazandağ M, Canpolat C, Malkondu O, Kaptan F, et al. Effect of acid ‐ etching procedure on selected physical properties of mineral trioxide aggregate. Int Endod J 2009; 42: 1004-1014.

29. Atabek D, Sillelioğlu H, Ölmez A. Bond Strength of Adhesive Systems to Mineral Trioxide Aggregate with Different Time Intervals. J Endod 2012; 38: 1288-1292.
30. Samimi P, Kazemian M, Shirban F, Alaei S, Khoroushi M. Bond strength of composite resin to white mineral trioxide aggregate: Effect of different surface treatments. J Conserv Dent 2018; 21: 350-353.
31. Gulati S, Shenoy VU, Margasahayam SV. Comparison of shear bond strength of resin-modified glass ionomer to conditioned and unconditioned mineral trioxide aggregate surface: an in vitro study. J Conserv Dent 2014; 17: 440-443.
32. Koç C, Aslan B, Ulusoy Z, Oruçoğlu H. Sealing ability of three different materials to repair furcation perforations using computerized fluid filtration method. J Dent Res Dent Clin Dent Prospects 2021; 15: 183-187.
33. Karabucak B, Li D, Lim J, Iqbal M. Vital pulp therapy with mineral trioxide aggregate. Dent Traumatol 2005; 21: 240-243.
34. Xavier MT, Costa AL, Caramelo FJ, Palma PJ, Ramos JC. Evaluation of the Interfaces between Restorative and Regenerative Biomaterials Used in Vital Pulp Therapy. Materials 2021; 14: 5055.
35. Bayrak S, Tunç ESen, Saroğlu I, Eğilmez T. Shear bond strengths of different adhesive systems to white mineral trioxide aggregate. Dent Mater J 2009; 28: 62-67.